11-1-1998

A Late Cambrian Positive Carbon-Isotope Excursion in the Southern Appalachians: Relation to Biostratigraphy, Sequence Stratigraphy, Environments of Deposition, and Diagenesis

Bosiljka Glumac
Smith College, bglumac@smith.edu

Kenneth R. Walker
The University of Tennessee, Knoxville

A LATE CAMBRIAN POSITIVE CARBON-ISOTOPE EXCURSION IN THE SOUTHERN APPALACHIANS: RELATION TO BIOSTRATIGRAPHY, SEQUENCE STRATIGRAPHY, ENVIRONMENTS OF DEPOSITION, AND DIAGENESIS

BOSILJKA GLUMAC[1] AND KENNETH R. WALKER[2]
[1] *Department of Geology, Smith College, Northampton, Massachusetts 01063, U.S.A.*
[2] *Department of Geological Sciences, The University of Tennessee, Knoxville, Tennessee 37996-1410, U.S.A.*

ABSTRACT: **A positive carbon-isotope excursion is recorded within the Upper Cambrian sedimentary succession in the southern Appalachians that consists of the Nolichucky Shale, the Maynardville Formation, and the Copper Ridge Dolomite. The lower part of the succession contains *Aphelaspis* zone fauna (Early Steptoean). The extensively dolomitized and poorly fossiliferous nature of the upper part of the succession precludes any detailed biostratigraphic determinations. Correlation with similar positive carbon-isotope excursions in coeval successions elsewhere suggests that this excursion represents a perturbation in the global cycling of carbon.**

Comparison of excursions at different localities in North America provides a means for the application of carbon-isotope stratigraphy. In the southern Appalachians the excursion started during deposition of the upper Nolichucky Shale. Maximum $\delta^{13}C$ values (4 to 5‰ PDB) are associated with the conformable interval at the Maynardville/Copper Ridge Dolomite transition, which has been interpreted as a correlative conformity in sequence-stratigraphic terms. The excursion ended during deposition of the lower Copper Ridge Dolomite. In western North America the excursion started at the base of the Pterocephaliid Biomere (near the base of the *Aphelaspis* Zone). This well-documented excursion ended prior to the end of the Pterocephaliid Biomere, with the maximum excursion at the Sauk II/Sauk III unconformity. This supports the correlation between Late Steptoean (Dresbachian/Franconian) sea-level fall and the sequence boundary at the end of Cambrian Grand Cycle deposition in the southern Appalachians.

The cause of this carbon-isotope excursion remains unclear. The excursion most likely reflects the enhanced burial of organic carbon promoted by ocean stratification, a warm nonglacial climate, and a sea-level maximum during the early Late Cambrian. The onset of regression may have contributed to the maximum carbon-isotope excursion by enhancing sedimentation rates, and by increasing organic productivity because of increased nutrient availability. The removal of carbon from the ocean surface may have caused a decrease in p_{CO_2} of the atmosphere. The resulting cooling episode could have triggered an oceanic overturn bringing ^{12}C-enriched bottom waters to the surface, which in conjunction with oxidation of organic matter during the sea-level fall, ended the carbon-isotope excursion.

Comparison of $\delta^{13}C$ and $\delta^{18}O$ values of matrix samples to the associated cement phases provides insights into the relationship between isotope variations and depositional and diagenetic environments. $\delta^{13}C$ values of peritidal dolomicrite define a rather smooth stratigraphic variation curve, whereas the values for subtidal micrite have significant scatter resulting from involvement of organic matter in diagenesis. Fibrous to bladed calcite cement from the subtidal deposits has $\delta^{13}C$ and $\delta^{18}O$ values comparable to the associated micrite, suggesting precipitation from marine water and similar diagenetic modifications. Meteoric diagenesis may be responsible for the depletion of ^{13}C and ^{18}O in equant calcite cement relative to the micrite. For saddle dolomite cement, the depletion of ^{18}O and $\delta^{13}C$ values similar to those for the peritidal dolomicrite, are consistent with formation during burial at elevated temperatures in a rock-dominated system.

This study demonstrates the potential of applying carbon-isotope stratigraphy, developed in highly fossiliferous successions, to stratigraphic intervals with poorly constrained biostratigraphy. Such studies require evaluation of the effects of depositional environments and diagenesis upon the preservation of marine isotope signatures.

INTRODUCTION

Carbon-isotope stratigraphy is a promising tool for high-resolution stratigraphy and correlation of successions that lack prominent biostratigraphic markers. This type of correlation has been applied to several Proterozoic and Neoproterozoic successions (Kaufman et al. 1992; Narbonne et al. 1994; Kaufman and Knoll 1995; Knoll et al. 1995a; Pelechaty et al. 1996; among others). In Mesozoic and Cenozoic successions, carbon-isotope stratigraphy has been used for basin-to-platform and regional correlation of strata beyond the current level of biostratigraphic resolution (e.g., Föllmi et al. 1994; Vahrenkamp 1996).

Because of relatively small effects of temperature and equilibrium carbon-isotope fractionation, variations in $\delta^{13}C$ values of carbonate minerals most commonly reflect changes in the $^{13}C/^{12}C$ ratio of the solution from which they precipitated (Anderson and Arthur 1983; Romanek et al. 1992). Accordingly, temporal fluctuations in $\delta^{13}C$ of marine carbonate constituents can represent secular variations of $\delta^{13}C$ in ocean water. Positive or negative excursions are of special interest in carbon-isotope studies. These excursions commonly occur at major boundaries throughout the stratigraphic record, and are indicators of tectonic, climatic, oceanographic, and evolutionary changes that influence carbon cycling (Magaritz 1991).

Upper Cambrian successions record a large, global, positive carbon-isotope excursion (Brasier 1993; Saltzman et al. 1998). Such excursions are normally interpreted as the result of one or a combination of the following factors: (1) an increase in organic productivity, and an associated increase in the fraction of carbon buried as organic matter during explosive evolutionary events; (2) increased sedimentation rates within oceans and associated increases in accumulation rates of organic matter; and (3) enhanced preservation of organic material caused by an expanded oxygen-minimum zone or marine anoxia (Weissert 1989; Derry et al. 1992; Brasier et al. 1994; Calvert et al. 1996; among others). Positive carbon-isotope shifts in any particular section or basin may also result from regional variations related to basin evolution (Beauchamp et al. 1987) or diagenetic alteration. Therefore, in order to fully constrain the anatomy of secular oceanic carbon-isotope fluctuations, it is necessary to evaluate the possible effects of local-to-regional depositional environments and diagenesis upon isotope signatures.

This paper presents results of a detailed study of carbon-isotope variations within an Upper Cambrian sedimentary succession of the southern Appalachians that includes the upper Nolichucky Shale and Maynardville Formation of the Conasauga Group and the lower part of the overlying Copper Ridge Dolomite of the Knox Group. This succession lacks prominent biomarkers, especially in the upper, extensively dolomitized part. Consequently, the biostratigraphy of this stratigraphic interval is poorly constrained. On the other hand, a detailed sequence-stratigraphic framework, with an emphasis on the Maynardville Formation, has been previously developed (Glumac 1997). In order to provide a more detailed chronostratigraphic framework for the deposition of this interval, carbon-isotope

JOURNAL OF SEDIMENTARY RESEARCH, VOL. 68, NO. 6, NOVEMBER, 1998, P. 1212–1222
 1073-130X/98/068-1212/$03.00

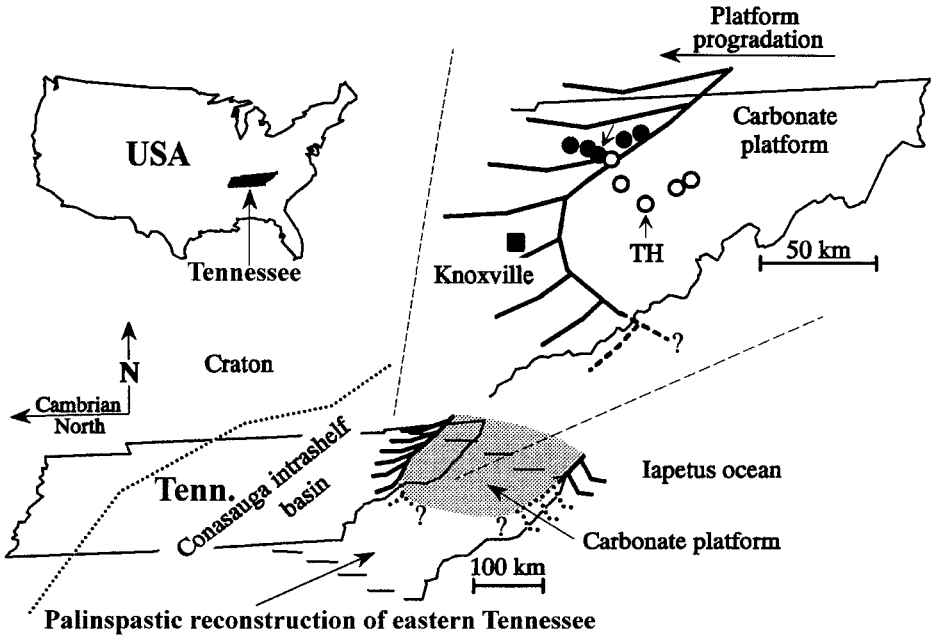

FIG. 1.—Schematic paleogeographic reconstruction of Tennessee during the early Late Cambrian. A carbonate platform (shaded area) faced the Iapetus ocean to the east (present-day orientation), and was separated from the exposed craton to the west by the Conasauga intrashelf shale basin (palinspastic reconstruction after Roeder and Witherspoon 1978). The area along the western carbonate platform margin is enlarged at upper right. Shown are the present-day (solid circles) and palinspastically reconstructed (open circles) locations of outcrops of Upper Cambrian deposits used for paleoenvironmental study (see Glumac 1997). Carbon-isotope stratigraphy was studied at the Thorn Hill (TH) outcrop (arrows).

stratigraphy was applied. The Maynardville Formation revealed a distinctive carbon-isotope pattern: $\delta^{13}C$ values of various diagenetic and depositional carbonate components are highly variable, but in general they are more positive or more enriched in ^{13}C than the underlying and the overlying strata (Glumac 1997). The anatomy of this positive carbon-isotope excursion was determined through extensive sampling at one of the most complete and best exposed outcrops of the lower Paleozoic sedimentary succession in the southern Appalachians (Fig. 1). These data were then compared with information available on time-equivalent, highly fossiliferous successions elsewhere. The effects of depositional environments on the carbon-isotope signature were evaluated by determining isotope compositions for samples from various lithofacies and by relating them to paleoenvironmental interpretations. The $\delta^{18}O$ values of individual depositional and diagenetic carbonate components were used to constrain the diagenetic environments and the extent of diagenetic modifications.

GEOLOGIC SETTING AND DEPOSITIONAL ENVIRONMENTS

The Conasauga Group (Middle to Upper Cambrian) alternating shale and carbonate units, or Grand Cycles, were deposited along the western margin of a carbonate platform separated from the craton by an intrashelf shale basin (Fig. 1). Early Late Cambrian progradation of the carbonate platform across the infilled intrashelf basin towards the craton marked the end of predominantly subtidal Grand Cycle deposition and establishment of peritidal carbonate deposition of the Knox Group (Upper Cambrian to Lower Ordovician; Fig. 1).

Paleoenvironmental interpretations are based on a detailed sedimentologic study by Glumac (1997) that focused on the Maynardville Formation (Fig. 1). The sedimentary succession records shallowing from subtidal mixed shale/carbonate deposition to peritidal carbonate deposition (Fig. 2). Subtidal deposition took place in a deep-ramp (upper Nolichucky) to shallow-ramp and lagoonal settings protected by localized ooid shoals and microbial (thrombolitic) patch reefs (lower Maynardville; Fig. 2). These subtidal environments were laterally linked to a broad, semiarid carbonate tidal flat, characterized by a variety of peritidal environments (upper Maynardville/Copper Ridge; Fig. 2). Subtidal carbonate deposits are dominated by ribbon rocks containing centimeter-scale limestone layers alternating with shale, or calcareous siltstone and argillaceous dolostone. The limestone layers consist of horizontally laminated and burrowed mudstone, peloidal wackestone/packstone, peloidal–fossiliferous packstone/grainstone, and less common intraclastic packstone (flat-pebble conglomerate). A gradual transition from ribbon rocks into microbially laminated deposits (stratiform stromatolites) marks the establishment of peritidal deposition (Fig. 2). The peritidal deposits contain a variety of extensively dolomitized lithofacies, among which centimeter-scale, normally graded couplets or mechanical laminites predominate (Fig. 2). Bases of coarse-grained couplets contain peloids, intraclasts, ooids, and quartz grains. Medium-grained couplets are composed of peloidal packstone grading upward into mudstone. Fine-grained couplets consist mainly of dolomitized mudstone. Couplets are interbedded with a variety of microbial deposits (Fig. 2).

The transition between the Maynardville and the Copper Ridge Dolomite is within a conformable interval that contains common sand-size siliciclastic detritus (quartz and K-feldspar; Fig. 2). This interval is interpreted as a correlative conformity linked to the Dresbachian/Franconian or Sauk II/Sauk III unconformity on the craton (Glumac 1997). An unconformity is absent in the southern Appalachians because the rate of passive-margin thermal subsidence exceeded the rate of sea-level fall (Bond et al. 1989; Osleger and Read 1993).

SAMPLING STRATEGY AND INVESTIGATIVE METHODS

Ideal samples for determining paleoceanic isotope compositions are unaltered abiotic marine cements precipitated as low-Mg calcite under oxic conditions and in isotopic equilibrium with their depositional environment (Lohmann and Walker 1989; Carpenter et al. 1991; Marshall 1992). Marine cements are not abundant in the Upper Cambrian succession examined, so this study relied on the use of fine-grained carbonate matrix composed of calcite or dolomite (Table 1). The potential of using shallow-water micrite and dolomicrite for the reconstruction of seawater carbon-isotope evolution has been documented by numerous authors (Fairchild et al. 1990; Magaritz et al. 1991; Marshall 1992; Schidlowski and Aharon 1992; Brasier et al. 1994; Kaufman et al. 1993; Narbonne et al. 1994; Kaufman and Knoll 1995; Knoll et al. 1995b).

Samples from the Nolichucky Shale and the subtidal package of the Maynardville were primarily collected from the micritic layers of the ribbon rocks (Table 1). Some of the samples came from micritic intraclasts comprising flat-pebble conglomerate, micritic lenses encased within packstone/grainstone layers, and intergranular areas of micrite-supported lithologies.

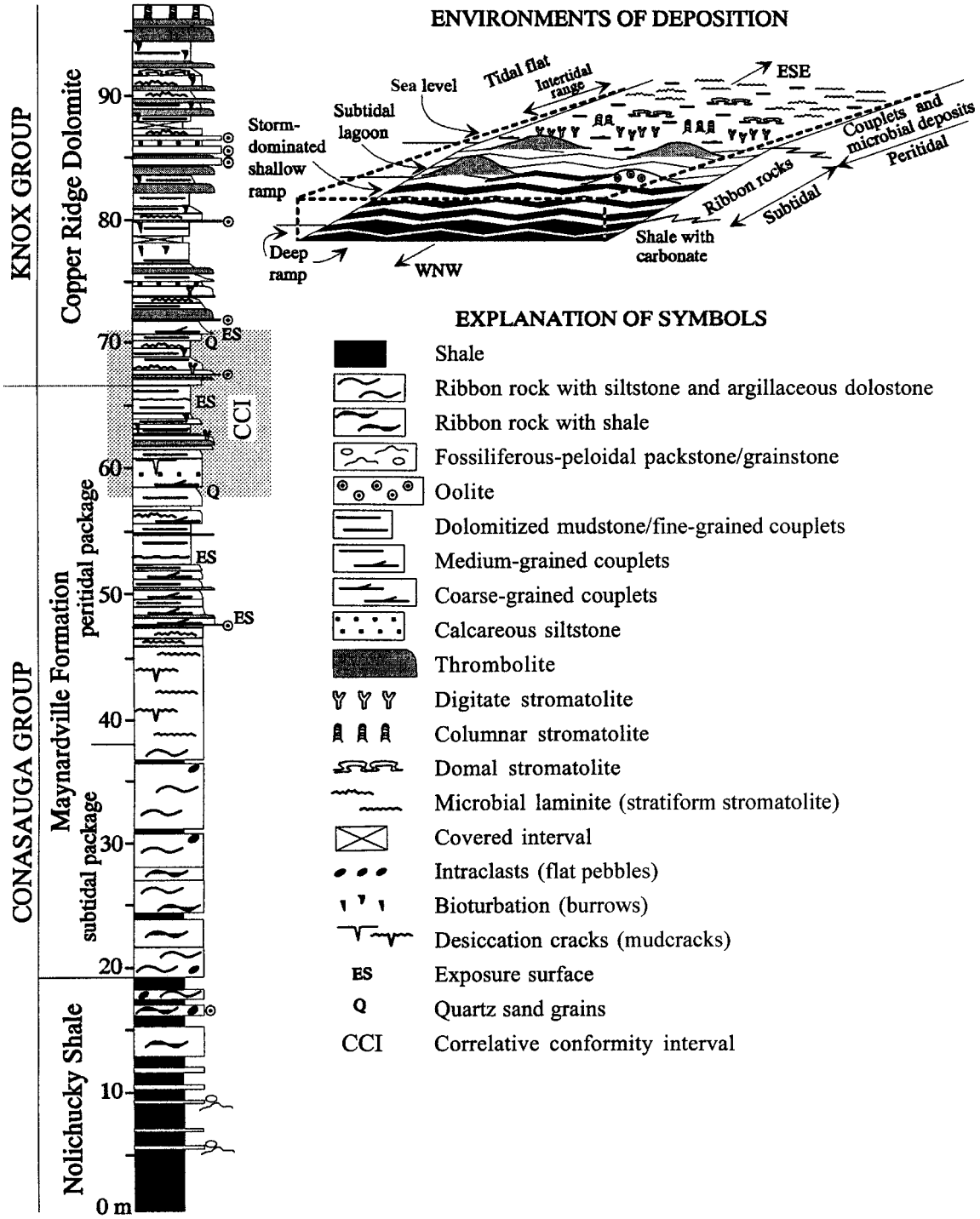

FIG. 2.—Stratigraphic column measured at the Thorn Hill outcrop (left), showing the Upper Cambrian sedimentary succession for which the variations in carbon-isotope ratios were determined. Note the position of the correlative conformity interval (CCI; shaded area) at the Maynardville/Copper Ridge transition (see text for additional explanation). Interpretation of environments of deposition is based on the study of five outcrops of this stratigraphic interval in northeastern Tennessee (see Figure 1).

The transition between the subtidal and peritidal packages is represented by micrite samples from microbial laminites or stratiform stromatolites (Table 1). These samples reflect a shift from calcite below to a predominance of dolomite in the peritidal deposits. Samples from the peritidal package of the Maynardville and the Copper Ridge Dolomite consist mainly of dolomicrite from mudstone, couplets, and microbial deposits (Table 1). Several samples were of dolomicrosparite, and rare more coarsely crystalline replacement dolomite. Samples of individual cement phases include fibrous to bladed calcite, equant calcite, and saddle dolomite (Table 2).

Samples for isotopic analysis were collected by drilling 2–10 mg of individual homogeneous carbonate depositional and diagenetic components from polished and stained thin-section billets using a microscope-mounted microdrill assembly after careful petrographic examination. The mineral composition of the collected material was checked using standard X-ray

diffraction methods. Organic matter was removed by roasting the powdered samples at 380°C for one hour. Samples were reacted off-line with 100% H_3PO_4 at 25°C for 24 hours (calcite) or 48 hours (dolomite). For mixed calcite/dolomite samples, a time extraction procedure was used (Epstein et al. 1963; Walters et al. 1972; Wada and Suzuki 1983). Isotope values were obtained on a VG-903 isotope ratio mass spectrometer and are reported as $\delta^{13}C$ and $\delta^{18}O$ in permil (‰) relative to the PDB standard. External precision was ±0.05‰ for both $\delta^{13}C$ and $\delta^{18}O$; sample reproducibility ($\pm 1\sigma$) was 0.2‰.

RESULTS OF STABLE-ISOTOPE ANALYSIS

Determined stratigraphic variations in carbon and oxygen isotope compositions are shown in Figure 3. The $\delta^{13}C$ values of subtidal micrite fluctuate greatly but in general show an increase from the upper Nolichucky into the subtidal deposits of the Maynardville. Dolomicrite samples from the peritidal package of the Maynardville and the Copper Ridge Dolomite form a smoother carbon-isotope variation curve. Some of the most positive $\delta^{13}C$ values correspond to the correlative conformity interval at the Maynardville/Copper Ridge transition (Fig. 3). The $\delta^{13}C$ values decline in the lower part of the Copper Ridge Dolomite. There is a poor correlation between the $\delta^{13}C$ and $\delta^{18}O$ values of matrix samples (Figs. 3, 4). In general, micrite samples are more depleted in ^{18}O ($\delta^{18}O = -9.3$ to -7.2‰ PDB) than dolomicrite ($\delta^{18}O = -8.1$ to -5.9‰ PDB).

In Figure 3 the data points representing the individual diagenetic phases are superimposed on the $\delta^{13}C$ and $\delta^{18}O$ stratigraphic variation trends. Data points for the fibrous to bladed calcite cement from the subtidal depositional package of the Maynardville plot within the $\delta^{13}C$ and $\delta^{18}O$ variation curve defined by micrite samples. Rare fibrous to bladed calcite from the Copper Ridge Dolomite has the most negative $\delta^{18}O$ value (−10‰ PDB), and is significantly depleted in ^{18}O relative to the associated dolomicrite. Equant calcite cement is depleted in both ^{13}C and ^{18}O in comparison to the micrite samples. The $\delta^{13}C$ values of saddle dolomite show a rather good correlation with the dolomicrite $\delta^{13}C$ variation curve, with some values being only slightly depleted in ^{13}C. On the other hand, saddle dolomite samples are generally depleted in ^{18}O in comparison to associated dolomicrite (Fig. 3).

EFFECTS OF DEPOSITIONAL ENVIRONMENTS AND DIAGENESIS ON CARBON-ISOTOPE SIGNATURES

Environmental Influence

The relatively short residence time of carbon in the oceans contributes to their isotopic heterogeneity (Holser et al. 1986). The carbon-isotope composition of modern oceans ranges between about −0.5 and +2.0‰ PDB (Kroopnick 1985). Therefore, carbon-isotope excursions of 1 to 2‰ are difficult to apply to the interbasinal correlation of strata in the absence of sufficient biostratigraphic control (Kaufman and Knoll 1995). The magnitude of the excursion documented in this study (4 to 5‰) is larger than the expected natural variation in oceanic carbon-isotope composition, and is consistent with a large perturbation in carbon cycling (Fig. 3).

Carbon-isotope stratigraphy is not applicable if isotope compositions correlate strongly with facies (Kaufman and Knoll 1995). There is no systematic variation between lithofacies and carbon-isotope values for the samples analyzed (Fig. 5). Data for the peritidal fine-grained couplets and dolomitized mudstone suggest that depositional environments alone cannot account for such a large (> 5.5‰) range of $\delta^{13}C$ values (Fig. 5). Mean $\delta^{13}C$ values for all peritidal lithofacies (microbial deposits and couplets) are similar (< 1‰ difference between four mean values; Fig. 5). These mean values are slightly higher than the mean value for the subtidal deposits (Fig. 5). This difference can be related to the large number of subtidal micrite samples from the Nolichucky Shale representing the period prior to the start of the excursion (Fig. 3). Possible depth-related variations in $\delta^{13}C$, however, could have produced a similar trend. The $\delta^{13}C$ composition of surface waters in modern oceans is highly variable, but is in general enriched in ^{13}C relative to deep ocean waters (by about 2‰), because of biological and air–sea exchange processes (Kroopnick 1985; Charles et al. 1993). Such depth-related variations most likely did not affect the Upper Cambrian deposits examined because they represent shallow-water deposition (Fig. 2). The deep-ramp carbonate deposits of the Nolichucky Shale are mostly allochthonous deposits remobilized from shallower parts of the platform (Fig. 2).

Modern marine hypersaline brines have wide variations in carbon-isotope compositions caused by evaporation, precipitation of $CaCO_3$, organic-matter decomposition, atmospheric CO_2 invasion, and biogenic effects of microbial mat communities (Stiller et al. 1985; DesMarais et al. 1989; Lazar and Erez 1992). Recognition of these effects is important for interpreting the isotope compositions of ancient carbonate deposits associated with evaporites and microbial deposits. Stiller et al. (1985) indicated that carbonate formed in association with evaporating brines should be enriched in ^{13}C as a result of non-equilibrium gas-transfer isotope fractionation caused by loss of CO_2 from the brines. Such processes could have contributed to the ^{13}C enrichment of the peritidal deposits of the Maynardville and the Copper Ridge Dolomite relative to the subtidal deposits (Fig. 3). The least negative $\delta^{13}C$ values correspond to dolomicrite samples from the correlative conformity interval, and are associated with a sea-level fall that could have caused enhanced evaporation (Fig. 3). Evaporite pseudomorphs are common in this part of the stratigraphic succession, but they are also present within the peritidal deposits with significantly lower $\delta^{13}C$ values. If extensive evaporation had been the primary cause for the ^{13}C enrichment, then an associated enrichment in ^{18}O would be expected. The maximum $\delta^{13}C$ values, however, are not paired with an increase in $\delta^{18}O$ values, and the decrease in $\delta^{13}C$ values in the Copper Ridge Dolomite is not accompanied by a decrease in $\delta^{18}O$ values (Fig. 3). This indicates that evaporitic conditions did not cause increased $\delta^{13}C$ values.

One might argue that vital effects could have possibly influenced the carbon-isotope composition of the Upper Cambrian microbial deposits. Photosynthetic fractionation of carbon by cyanobacteria is dependent on CO_2 availability, growth rate, cell size, and population density (Goericke et al. 1994). $\delta^{13}C$ values of dolomicrite from the microbial deposits are comparable to that of non-microbial micrite from the peritidal package, indicating the absence of significant vital influence (Table 1; Figs. 3, 5). This might have been predicted if one assumed that these stromatolites formed by trapping micritic particles that were derived from the same sediment source as the non-microbial micrite. The predicted and observed relationships are consistent with the lack of measurable vital effects in Proterozoic and Lower Cambrian microbial deposits, as determined from comparison with marine cements (Fairchild et al. 1990; Surge et al. 1997).

In summary, it is unlikely that variations in environmental conditions alone could have caused the positive carbon-isotope excursion, because of a general lack of correlation between lithofacies and the observed $\delta^{13}C$ trend. Minor variations in $\delta^{13}C$, superimposed on the general trend, may in part be related to varying environmental factors.

Diagenetic Influence

The diagenetic processes capable of causing changes in the carbon-isotope composition of marine carbonate components include neomorphism and recrystallization, reequilibration with fluids of differing isotope composition, and precipitation of isotopically different diagenetic carbonate phases (Veizer 1983; Fairchild et al. 1990; Kaufman et al. 1991; Marshall 1992; among others). The carbon-isotope value of marine organic matter is about 25‰ more negative than inorganic bicarbonate (Marshall 1992). Thus, degradation of organic matter has the potential to significantly alter the carbon-isotope composition of marine carbonate sediment. Reactions of organic-matter degradation include microbially mediated reduction of

TABLE 1.—*Stable-isotope data for matrix samples.*

Stratigraphic Position (m)	Description	$\delta^{18}O$ (‰PDB)	$\delta^{13}C$ (‰PDB)
NOLICHUCKY SHALE			
1.15	micrite between skeletal fragments of a thin limestone layer interbedded with shale	−8.52	0.16
3.05	micrite between skeletal fragments and from lenses/patches of a thin packstone/grainstone layer	−9.06	1.12
7.05	micrite from patches and between skeletal fragments of a wackestone/grainstone layer	−8.96	0.27
7.85	micrite from a nodular layer interbedded with shale	−8.47	0.89
11.85	micrite from lenses and in between skeletal fragments of a packstone/grainstone layer	−8.03	0.33
13.75	micrite from a mudstone layer interbedded with argillaceous layers of ribbon rocks	−9.34	0.53
15.0	micrite from a mudstone layer interbedded with argillaceous layers of ribbon rocks	−8.10	0.97
16.7	micrite from mudstone layers/lenses interbedded with intraclastic and skeletal layers of ribbon rocks	−8.04	1.37
17.2	micrite from one small flat pebble incorporated within a skeletal packstone/grainstone layer	−8.06	1.13
18.25	micrite from a mudstone layer with nodular appearance imbedded within ribbon rocks	−7.95	1.18
MAYNARDVILLE FORMATION (MICRITE)			
19.6	micrite from intraclasts and patches in a fossiliferous-intraclastic packstone layer of ribbon rocks	−8.98	1.98
20.0	micrite from a mudstone layer of ribbon rocks	−8.84	2.54
21.1	micrite from burrow-mottled ribbon rocks	−7.90	3.01
22.15	micrite from a laminated mudstone layer of ribbon rocks	−7.48	1.82
23.35	micrite from a mudstone layer of ribbon rocks	−7.43	1.66
24.2	micritic matrix in between trilobite fragments from a limestone layer of ribbon rocks	−8.03	1.29
25.2	micrite from intraclasts (flat pebbles) in argillaceous dolomicritic layers of ribbon rocks	−7.87	0.49
25.4	micrite from a lense interbedded within argillaceous dolomicrite of ribbon rocks	−7.79	1.19
26.4	micrite from a mudstone to peloidal mudstone layer of ribbon rocks	−7.51	1.53
28.0	micrite in between trilobite fragments in fossiliferous wackestone/packstone of ribbon rocks	−7.43	1.13
29.0	time-extracted calcite component from argillaceous dolomicrite/calcareous siltstone	−8.23	2.35
30.05	micrite from a mudstone layer interbedded within argillaceous dolomicrite of ribbon rocks	−7.77	2.92
31.3	micrite from a mudstone layer underlying flat pebble conglomerate of ribbon rocks	−7.76	1.71
31.75	time-extracted calcite component from argillaceous dolomicrite/calcareous siltstone	−8.92	1.98
31.9	micrite from a mudstone/peloidal layer of ribbon rocks	−8.14	3.18
32.6	micrite from a lense within ribbon rocks	−7.48	3.21
33.45	micrite from a lense within ribbon rocks	−7.16	3.54
34.65	micrite from a mudstone layer of ribbon rocks	−7.58	4.09
36.75	micrite from a mudstone layer of ribbon rocks	−7.80	2.29
37.85	micrite to peloidal packstone from lenses in ribbon rocks	−7.63	3.52
38.8	micrite from burrowed lenses from transitional interval between ribbon rocks and microbial deposits	−7.88	3.80
40.5	micrite from microbial laminites; contains about 30% dolomicrite; time extraction used	−8.63	3.39
42.2	micrite from microbial laminites; contains about 10% dolomicrite; time extraction used	−8.73	3.68
43.45	micrite from microbial laminites; contains common dolomicrite; time extraction used	−8.91	3.41
MAYNARDVILLE FORMATION (DOLOMICRITE)			
45.55	dolomicritic laminae from stratiform stromatolites	−6.58	3.90
46.6	dolomicritic laminae from stratiform stromatolites	−6.21	4.01
47.8	dolomicrite from a layer overlying microbially laminated deposits	−6.41	3.25
48.35	dolomicrite from upper parts of coarse-grained couplets	−6.76	2.76
49.6	dolomicrite from fine-grained couplets	−7.02	2.72
50.7	dolomicrite from fine-grained couplets	−7.41	2.46
50.7	dolomicrosparite from fine-grained couplets	−7.23	2.66
51.4	dolomicrosparite from fine/medium-grained couplets	−8.07	3.01
52.9	dolomicrite from upper parts of fine/medium-grained couplets	−7.07	3.03
53.1	dolomicrite from fine-grained couplets	−7.05	3.01
53.1	dolomicrite from mudstone	−7.88	3.25
53.35	dolomicrite from mudstone; 5 cm below a prominent exposure surface	−7.29	3.28
53.4	dolomicrite from clasts in topographic lows immediately above the exposure surface	−7.77	3.25
53.4	dolomicrite from clasts in topographic lows immediately above the exposure surface	−7.67	3.18
53.42	dolomicrite from a lamina in the shaly interval deposited on the exposure surface	−7.64	2.97
53.43	laminated dolomicrite from fine-grained couplets with mudcracks; 5 cm above the exposure surface	−7.72	3.08
53.45	dark argillaceous dolomicritic matrix from a shaly interval deposited on the exposure surface	−7.77	3.26
54.6	dolomicrite from mudstone	−6.82	3.68
55.6	dolomicrite from mudstone/fine-grained couplets	−6.12	3.06
56.55	dolomicrite from upper parts of medium-grained couplets with common desiccation cracks	−6.96	2.88
57.6	dolomicrite from fine/medium-grained couplets with desiccation cracks	−6.39	2.96
CORRELATIVE CONFORMITY INTERVAL			
58.7	dolomicrite from mudstone	−6.59	3.14
59.05	dolomicrite from upper parts of fine/medium-grained couplets	−5.86	3.43
60.25	dolomicrite from upper parts of medium-grained couplets	−6.35	3.82
61.15	dolomicrite from upper, burrowed parts of medium-grained couplets	−5.99	3.80
61.9	dolomicrite from upper parts of medium-grained couplets	−6.99	3.61
63.3	slightly laminated dolomicrite from mudstone/very fine-grained couplets	−6.87	3.76
63.8	dolomicrosparite from burrowed mudstone	−6.55	4.78
64.75	dolomicrosparite from burrowed mudstone/fine-grained couplets	−6.38	4.30
65.7	dolomicrosparite from slightly burrowed mudstone/fine-grained couplets	−6.36	3.94
67.1	dolomicrite from fine-grained couplets/mudstone	−6.18	3.40
67.7	dolomicrosparite from microbial laminites	−8.00	3.69
68.9	dolomicrite from microbial laminites	−6.78	3.55
70.0	dolomicrite from burrowed mudstone/fine-grained couplets	−6.24	4.08
70.7	dolomicrite from mudstone/fine-grained couplets; abundant quartz sand grains and evaporites	−6.33	3.83
71.75	laminated dolomicrite from fine-grained couplets	−6.68	3.11

TABLE 1.—*Continued.*

Stratigraphic Position (m)	Description	$\delta^{18}O$ (‰PDB)	$\delta^{13}C$ (‰PDB)
COPPER RIDGE DOLOMITE			
72.75	laminated dolomicrite from microbial ''lumps'' imbedded within deposits with thrombolitic texture	−6.55	2.94
73.9	dolomicrite to dolomicrosparite from burrowed fine-grained couplets	−6.54	3.02
74.8	dolomicrite to dolomicrosparite from mudstone	−6.55	2.31
75.25	dolomicrite from upper micritic part of coarse-grained couplets	−5.99	2.65
76.8	dolomicrite from fine-grained couplets	−6.38	2.20
77.25	dolomicrite from fine-grained couplets	−7.44	2.42
78.15	dolomicrite from burrow-mottled mudstone/fine-grained couplets	−6.43	3.71
79.35	medium-crystalline replacement dolomite; original lithology: bioturbated couplets?	−6.40	3.16
80.4	dolomicrite from stratiform stromatolite laminae	−6.37	2.72
81.4	dolomicrite from fine to medium-grained couplets	−7.13	2.77
82.45	dolomicrite from microbial laminites or digitate stromatolites	−6.42	2.36
83.5	dolomicrosparite from bioturbated peloidal packstone/wackestone	−6.49	2.66
85.3	dolomicrosparite/medium-crystalline replacement dolomite from mudstone above thrombolite	−6.09	2.45
86.9	dolomicrite from fine-grained couplets overlying domal stromatolites	−6.36	1.42
87.25	dolomicrite from fine-grained couplets	−6.64	1.42
88.35	dolomicrosparite from mottled (burrowed) mudstone	−6.52	1.78
89.3	dolomicrite from undisturbed parts of mottled medium-grained couplets	−6.18	1.64
90.2	dolomicrite from upper part of medium-grained couplets	−6.38	0.83
91.45	dolomicrite from relatively undisturbed parts of mottled fine/medium-grained couplets	−7.08	0.79
92.55	dolomicrite from relatively undisturbed parts of mottled mudstone	−6.86	−0.07
93.25	dolomicrite from mudstone	−7.31	−0.85
94.15	dolomicrite from mudstone	−6.70	0.09

iron, manganese, sulfate, and nitrate under suboxic conditions, and methanogenesis under anoxic conditions with subsequent abiogenic thermal decarboxylation processes at increased temperature during burial (Claypool and Kaplan 1974; Irwin et al. 1977; Coleman and Raiswell 1981; Winter and Knauth 1992). Most of these reactions release organogenic carbon, which decreases the $\delta^{13}C$ value of dissolved bicarbonate and any precipitated carbonate phases. The exception is ^{13}C-enriched CO_2 that forms during degradation of organic matter by methanogenic bacteria due to kinetic fractionation between methane and CO_2 (Irwin et al. 1977). Positive $\delta^{13}C$ values (up to +15‰ PDB) of carbonate minerals may therefore represent precipitation during methanogenesis. The products of different reactions of organic-matter degradation are commonly mixed with each other and with dissolved marine bicarbonate, thereby producing a wide range of carbon-isotope compositions of pore fluids and resulting carbonate mineral phases (Gautier and Claypool 1984; Iyer et al. 1995). Massive alteration or the resetting of $\delta^{13}C$ values in existing carbonate phases during diagenesis, however, is hindered by small concentrations of carbon in the diagenetic fluids (Banner and Hanson 1990). The carbon-isotope composition of porewater is commonly controlled by the composition of the dissolving carbonate phase. Carbonate $\delta^{13}C$ values can be modified only in very open systems (high fluid–rock ratio) or in the presence of brines with elevated levels of total dissolved carbon (Banner and Hanson 1990).

The majority of samples used in this study are homogeneous micrite and dolomicrite, without visible cements and skeletal fragments (Table 1). The samples predominantly have nonluminescent to dark, dully cathodoluminescence (CL) patterns, but in some cases exhibit a patchy distribution of nonluminescence to bright luminescence, suggesting possible diagenetic modification. Examples of diagenetic alteration in these deposits include neomorphism and recrystallization of micrite to microsparite, and dolomitization of fine-grained carbonate to dolomicrosparite and coarse-crys-

TABLE 2.—*Stable-isotope data for individual diagenetic components.*

Stratigraphic Position (m)	Description	$\delta^{18}O$ (‰PDB)	$\delta^{13}C$ (‰PDB)
20.55	fibrous/bladed calcite cement in between intraclasts of flat pebble conglomerate	−7.86	2.88
20.55	fibrous/bladed calcite cement in between intraclasts of flat pebble conglomerate	−7.80	2.97
34.0	ferroan equant calcite cement in voids (burrows?) within a micritic layer of ribbon rocks	−9.68	2.27
38.8	ferroan equant calcite cement in voids (burrows likely) within ribbon rocks	−9.07	2.70
39.1	ferroan equant calcite cement from burrows in microbially laminated deposits	−9.69	2.69
48.6	saddle dolomite cement from voids and fractures in deposits with remnant thrombolitic fabric	−8.60	3.14
51.5	saddle dolomite cement in large dissolutional or dissolution enlarged void in couplets	−8.10	2.80
52.05	saddle dolomite cement from voids in fine-grained couplets	−8.60	2.59
56.55	saddle dolomite cement in desiccation cracks in medium-grained couplets	−8.74	2.75
71.2	saddle dolomite cement from tectonic veins	−8.00	3.24
74.0	pore-central equant calcite cement in a void within micritic layer	−9.84	1.54
74.0	saddle dolomite cement from voids (desiccation?) in between intraclasts in limestone deposits	−7.01	2.77
74.2	saddle dolomite cement from microbial deposits (digitate stromatolites)	−6.98	2.63
74.4	saddle dolomite cement from microbial deposits (digitate stromatolites)	−6.88	2.87
75.4	fibrous/bladed calcite cement between micritic intraclasts of limestone deposits	−9.96	2.65
76.05	saddle dolomite cement between angular clasts of coarse-crystalline replacement dolomite	−6.92	2.68
76.05	saddle dolomite in argillaceous/bituminous matrix in burrows of microbial (thrombolitic) deposits	−6.73	2.68
79.35	saddle dolomite cement in voids (desiccation?, burrows?) within dolomitized couplets	−8.42	2.46
79.35	saddle dolomite embedded in bituminous matrix; from patches in mudstones or couplets	−6.65	2.90
83.5	saddle dolomite in argillaceous/bituminous matrix of burrows in mudstones/fine-grained couplets	−6.44	2.64
83.7	saddle dolomite cement in voids in dolomitized microbial (thrombolitic) deposits	−7.77	1.93
84.6	dolomite cement from intergranular pores of ooid grainstone deposit	−6.59	2.05
85.0	saddle dolomite cement in voids in dolomitized microbial (thrombolitic) deposits	−6.96	1.80
85.3	saddle dolomite cement in layer-parallel voids in microbial (thrombolitic) deposits	−7.33	1.66
85.55	dolomite cement in pores between dolomitized angular peloids	−7.39	1.75
88.75	saddle dolomite cement from voids in dolomitized and partially silicified microbial deposits	−7.17	1.27
93.4	saddle dolomite cement from bed-perpendicular fractures in couplets	−7.01	−0.61

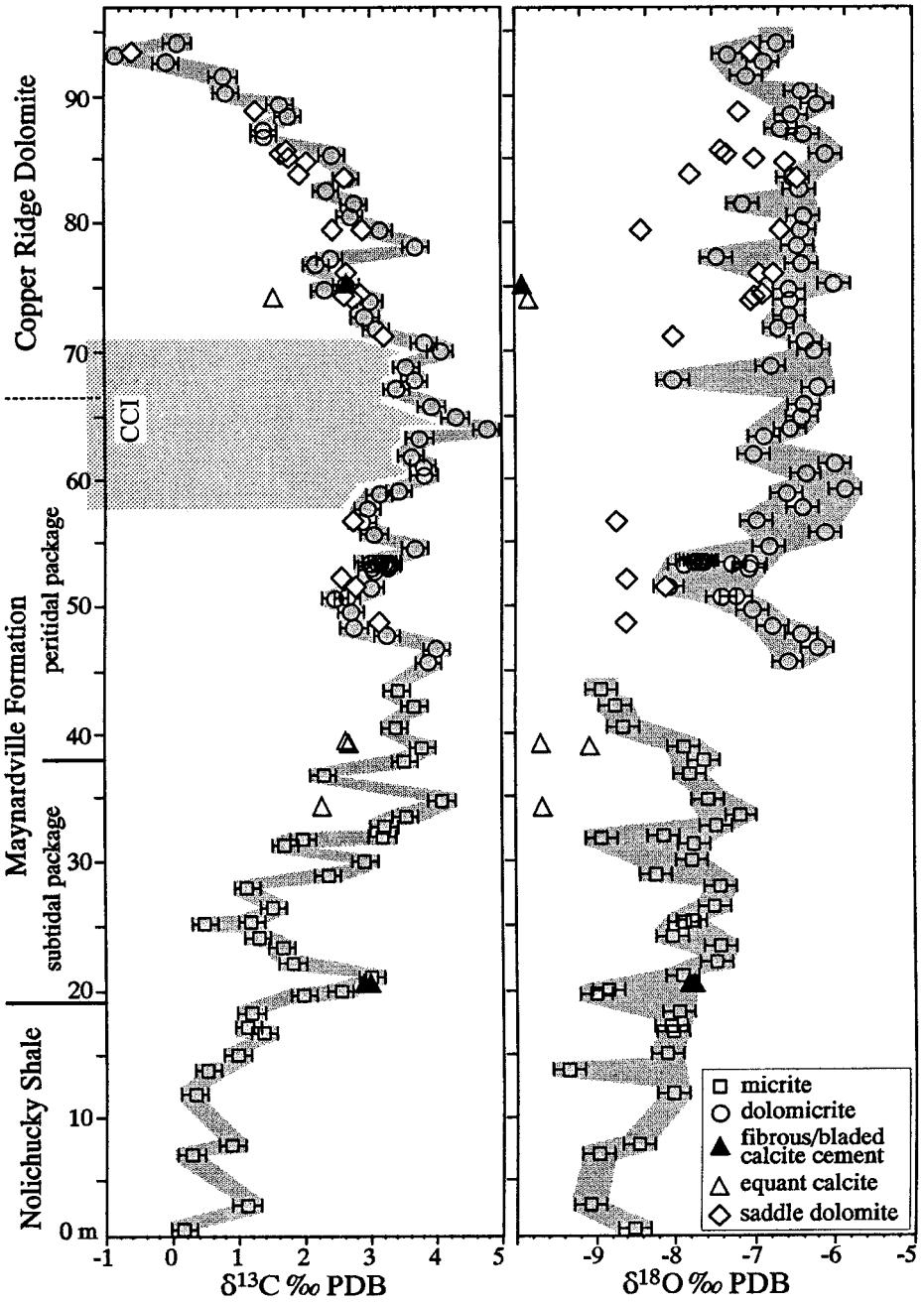

FIG. 3.—Variations in $\delta^{13}C$ and $\delta^{18}O$ values as a function of stratigraphic position of the samples. Isotope variation curves are constructed by connecting all measured isotope ratios for the micrite and dolomicrite samples. The width of the curves approximates a 0.2‰ reproducibility shown as horizontal error bars. Superimposed on the carbon-isotope variation curve are data points that represent the isotope compositions of individual diagenetic phases (see legend lower right). See Tables 1 and 2 for description of samples. The correlative conformity interval (CCI) at the Maynardville/Copper Ridge Dolomite transition is indicated. Note the poor correlation between $\delta^{13}C$ and $\delta^{18}O$ values, and the difference in $\delta^{18}O$ values between micrite and dolomicrite (see also Figure 4).

talline replacement dolomite (Glumac 1997). Diagenetic modifications are substantiated by oxygen-isotope compositions that are more negative than the predicted Cambrian marine calcite value of about −5.0‰ PDB (Figs. 3, 4; Lohmann and Walker 1989).

Superimposed on the general stratigraphic trend of increasing carbon-isotope values for the subtidal micrite in the lower Maynardville Formation is a wide scatter of $\delta^{13}C$ values (Fig. 3). Diagenesis in the presence of degrading organic matter can explain this data scatter. This is substantiated by the association of these deposits with framboidal pyrite, ferroan carbonate phases, skeletal fragments, bioturbation, and shale deposits that may have been rich in organic matter (Fig. 2). The increase in $\delta^{13}C$ values within the subtidal deposits is accompanied by a decrease in the amount of shale (Figs. 2, 3) but is not associated with any apparent diagenetic changes that could have caused the observed shift in the carbon-isotope signature. Therefore, the recorded shift is consistent with a secular trend in the marine $^{13}C/^{12}C$ increase. The less-scattered $\delta^{13}C$ values of the peritidal dolomicrite correspond to less common indicators for the presence of organic matter, and to the paucity of ferroan carbonate phases in these deposits (Fig. 3). The decline in $\delta^{13}C$ values within the Copper Ridge Dolomite is associated with neither changes in lithologic content nor diagenetic patterns, and thus also supports a secular trend.

Lack of systematic covariance between $\delta^{13}C$ and $\delta^{18}O$ values is commonly used as evidence that the carbon-isotope signal is not controlled by diagenetic alterations (Figs. 3, 4; Hudson and Anderson 1989; Derry et al. 1992; Brasier et al. 1994). The ^{18}O depletion in the samples analyzed, relative to estimated Cambrian marine calcite values, indicates alteration in the presence of meteoric waters and/or during burial at elevated temperature (Figs. 3, 4). Oxygen-isotope values of the peritidal dolomicrite are, in gen-

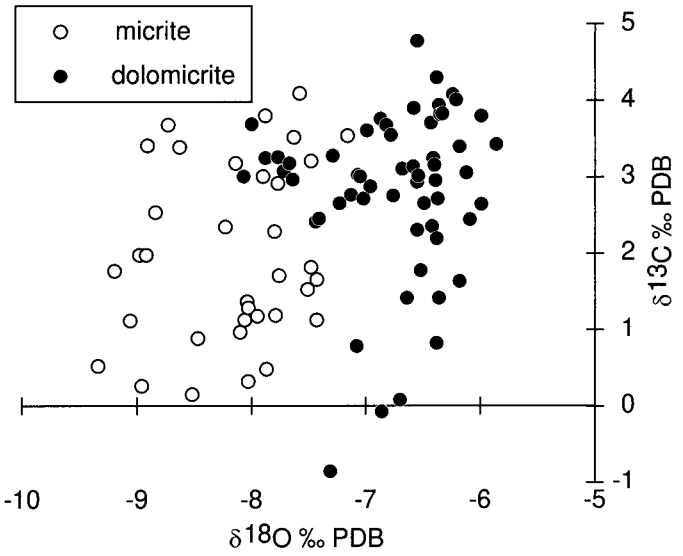

FIG. 4.—$\delta^{13}C$ versus $\delta^{18}O$ values for the micrite and dolomicrite samples.

eral, more enriched in ^{18}O relative to subtidal micrite (Figs. 3, 4). This can be explained by: (1) an equilibrium fractionation between dolomite and calcite (Friedman and O'Neil 1977; Land 1980); (2) formation of penecontemporaneous dolomite under sabkha-like evaporative conditions (McKenzie 1981); and (3) a lesser degree of later diagenetic alteration of dolomite relative to calcite (Knoll et al. 1995b). The ^{18}O depletion of dolomicrite samples, relative to estimated normal-marine Cambrian dolomite (assuming a $3 \pm 1‰$ enrichment relative to Cambrian marine calcite; Friedman and O'Neil 1977; Land 1980), is indicative of diagenetic alteration (Figs. 3, 4). The difference between the $\delta^{18}O$ values of micrite and dolomicrite samples is a function of differences in precursor carbonate compositions and styles of diagenetic modification.

Comparison of isotope compositions between carbonate matrix and associated cements provides insights into diagenetic environments and the extent of diagenetic modifications (Fig. 3). Similarity of $\delta^{13}C$ and $\delta^{18}O$ values for the fibrous to bladed calcite cement from the subtidal deposits and associated micrite suggests formation from marine water and similar diagenetic modification (Fig. 3). Depletion of ^{18}O in the fibrous to bladed calcite cement relative to the peritidal dolomicrite may be the result of meteoric diagenesis or may reflect later burial alteration. During diagenetic modification, the $\delta^{13}C$ value for fibrous to bladed calcite was buffered to the host-rock composition (Fig. 3). Precipitation from meteoric water may have been responsible for the depletion of ^{18}O and ^{13}C in the equant calcite cement relative to the associated matrix samples (Fig. 3). Equant calcite cement from the Maynardville Formation is ferroan in composition, and is associated with burrows. This suggests the possibility of incorporation of ^{13}C-depleted organogenic carbon into the equant calcite cement under reducing conditions in meteoric–phreatic or burial environments. The $\delta^{18}O$ values of saddle dolomite are comparable with, or more negative than, those of the associated dolomicrite, whereas their $\delta^{13}C$ compositions are comparable (Fig. 3). These observations are consistent with formation of saddle dolomite during burial at elevated temperatures in a rock-dominated system.

RELATION OF CARBON-ISOTOPE EXCURSION TO BIOSTRATIGRAPHY AND SEQUENCE STRATIGRAPHY

Biostratigraphic correlation of Cambrian strata is commonly limited, because of restricted geographic distribution and low preservation potential of many fossil taxa (Brasier 1993). Carbon-isotope stratigraphy, developed for Cambrian carbonate platform successions with a well-constrained biostratigraphic and sequence-stratigraphic framework, has great potential as a stratigraphic tool (Brasier 1993). Therefore, $\delta^{13}C$ variations for the Upper Cambrian of the southern Appalachians are compared with those for several coeval, biostratigraphically well-characterized successions (Brasier 1993; Saltzman et al. 1998).

The presence of *Cedaria* and *Crepicephalus* zone fauna has been reported in the Nolichucky Shale of northeastern Tennessee (Fig. 6; Bridge 1956; Derby 1965; Rasetti 1965). *Aphelaspis* zone fauna in the lower part of the Maynardville Formation (subtidal depositional package) constrains its age to the Dresbachian or Steptoean (Fig. 6). The base of the Maynardville is at or above the lower boundary of the *Aphelaspis* Zone (Fig. 6; Derby 1965). Traditionally, the base of the Maynardville is placed at the base of the first thick-bedded limestone unit above the Nolichucky Shale (Fig. 2), and as such it represents a facies boundary that may be diachronous. The upper part of the Maynardville (peritidal depositional package), and overlying Copper Ridge Dolomite deposits are extensively dolomitized and poorly fossiliferous. Trempealeauan fauna has been documented from the upper part of the Copper Ridge Dolomite (Bridge 1956; Derby 1965), but to date, no fossil of Franconian age has been identified in the southern Appalachians. Therefore, the Copper Ridge Dolomite has been considered to represent most of the Franconian and Trempealeauan stages (*Elvinia* to *Saukia* zones) of the Late Cambrian (Fig. 6; Bridge 1956; Rasetti 1965; Derby 1965; Osleger and Read 1993).

Brasier (1993) and Saltzman et al. (1998) reported a positive carbon-

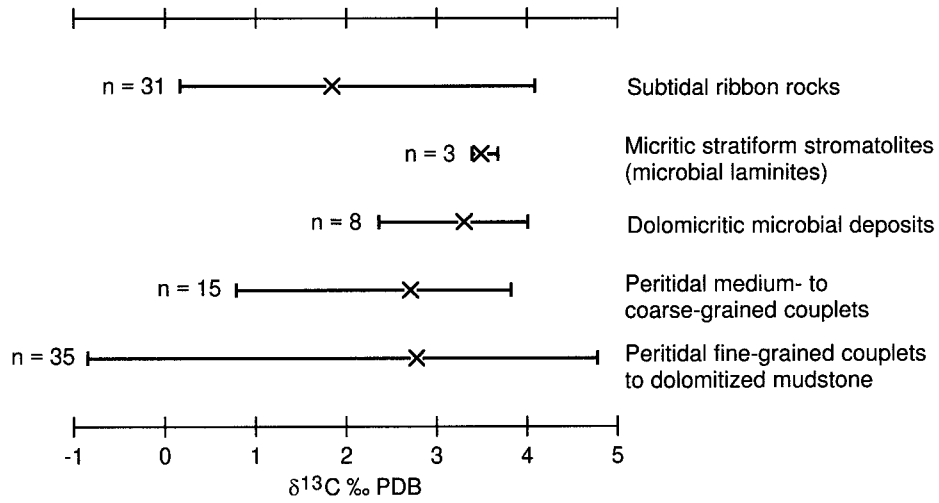

FIG. 5.—Ranges of $\delta^{13}C$ values for various lithofacies studied. The number of samples (n) and mean values (X) are indicated for each lithofacies.

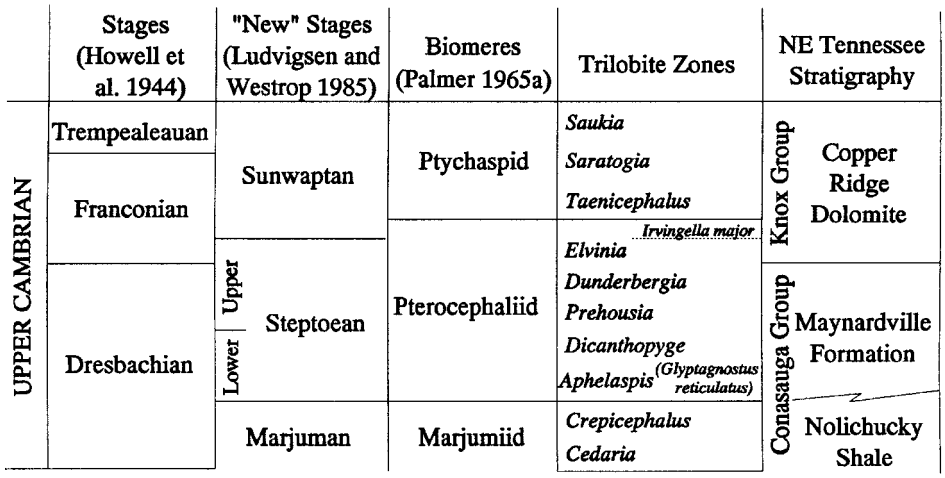

FIG. 6.—Upper Cambrian stratigraphy of the southern Appalachians in northeastern Tennessee. Interpretation is in part based on carbon-isotope stratigraphy because of the poorly fossiliferous and extensively dolomitized parts of this sedimentary succession (see text for details).

isotope excursion for the Upper Cambrian in the western United States (the Great Basin area), China, Kazakhstan, and Australia, suggesting that this is a widespread (possibly global) phenomenon. The beginning of the excursion is marked by an increase in $\delta^{13}C$ values of marine carbonate above a background range of -1 to $+1$‰ PDB. This increase is coincident with the first occurrence of the trilobite *Glyptagnostus reticulatus*, which corresponds to the base of the Pterocephaliid Biomere, the Steptoean Stage, and the *Aphelaspis* Zone (Fig. 6). This interval can be correlated worldwide as a marine extinction horizon at the Marjumiid–Pterocephaliid Biomere boundary (Ludvigsen and Westrop 1985). Maximum $\delta^{13}C$ values (4 to 5‰ PDB) correspond to the late Steptoean or Dresbachian/Franconian boundary interval, which is commonly represented by a craton-wide hiatus separating the Sauk II and Sauk III sequences. This part of the positive carbon-isotope excursion also coincides with maximum faunal diversity within the Pterocephaliid Biomere, which spans the late *Dunderbergia* to early *Elvinia* trilobite biozones (Palmer 1965b; Rowell and Brady 1976; Saltzman 1996).

Comparison with carbon-isotope excursions at other localities suggests that the start of the excursion in the southern Appalachians coincides with the base of the *Aphelaspis* Zone and Pterocephaliid Biomere in the upper Nolichucky (Figs. 3, 6). The return to background $\delta^{13}C$ values occurs in the lower Copper Ridge Dolomite (Fig. 3). This shift is known to occur prior to the end of the Pterocephaliid Biomere and during the *Elvinia* Zone (Saltzman et al. 1998), thus supporting an early Franconian or late Steptoean age for the lowermost Knox Group in the southern Appalachians (Fig. 6). This demonstrates the potential of using carbon-isotope stratigraphy to correlate stratigraphic successions for which detailed biostratigraphic determinations cannot be made. Such interpretations are possible, judging by the documented consistent relationships between carbon-isotope excursions and biostratigraphic markers on different continents (Gale et al. 1993), but should be made with a great degree of caution. Saltzman (1996), for example, noted that the Steptoean excursion started slightly earlier in China than in the Great Basin.

The maximum carbon-isotope excursion in the southern Appalachians corresponds with the occurrence of common siliciclastic detritus (Figs. 2, 3). The coincidence of the maximum carbon-isotope excursion and the sea-level lowstand in the western United States supports the interpretation that this interval represents the correlative conformity associated with the craton-wide Dresbachian/Franconian unconformity or Sauk II/Sauk III hiatus (Fig. 6). The maximum carbon-isotope excursion is coincident with widespread influx of siliciclastics during the *Dunderbergia* (late Dresbachian) and/or early *Elvinia* (early Franconian) faunal zones in the Great Basin as well (Saltzman et al. 1998).

The geometry of carbon-isotope curves can be used as an indicator of relative sediment accumulation rates and the distribution of discontinuities in the geologic record (Magaritz 1991; Pelechaty et al. 1996). For example, the thickness of the stratigraphic interval that records the Steptoean positive carbon-isotope excursion in the Great Basin of Nevada is in excess of 200 m (Saltzman et al. 1998). In comparison, the carbon-isotope excursion in the southern Appalachians is contained within about an 80 m thick succession (Fig. 3), implying a rather low sediment accumulation rate. An even more condensed interval is reported from passive-margin successions of the northern Appalachians of western Newfoundland, where the upper four Dresbachian trilobite zones (*Aphelaspis*, *Dicanthopyge*, *Prehousia*, and *Dunderbergia*) occur in less than 20 m of strata associated with thin layers of quartz sand (James and Stevens 1986).

POSSIBLE CAUSES AND CONSEQUENCES OF THE EXCURSION

A positive $\delta^{13}C$ shift of 4 to 5‰ in marine carbonate could be related to the removal of 20–25% organic carbon from ocean water (Berger and Vincent 1986). It has been postulated that accumulation of organic-rich sediment in the Phanerozoic was at its maximum during the early Paleozoic, with the Middle to Late Cambrian being one of the main episodes of deposition of organic-rich shale (Thickpenny and Leggett 1987). The Cambrian was a time of relatively warm global climate, characterized by sluggish, global ocean-current circulation that favored ocean stratification and the formation of anoxic deep waters (Wilde and Berry 1984; Weissert 1989). Sea level was at one of its maxima on the Laurentian craton during the *Cedaria* through *Aphelaspis* faunal zones in the early Late Cambrian (Fig. 6; Bond et al. 1988). High sea level contributes to salinity stratification and decreased terrestrial runoff, which can cause nutrient depletion and reduced organic productivity (Brasier 1992). This may have created nutrient-starved waters over anoxic bottom waters during the Cambrian along the margins of Laurentia (Brasier 1992).

This sea-level maximum was followed by regression and the widespread Dresbachian/Franconian or Sauk II/Sauk III hiatus (Lochman-Balk 1971; Palmer 1971, 1981; Bond et al. 1988; Osleger and Read 1993). Terrestrial runoff during sea-level fall increases nutrient influx, thus resulting in greater organic productivity and ^{12}C depletion of surface waters (Brasier 1992). High trilobite and brachiopod diversity during the late *Dunderbergia* Zone (Rowell and Brady 1976) does not necessarily imply high organic productivity. In the absence of direct evidence for an increase in organic productivity, the Late Cambrian positive carbon-isotope excursion can be explained by an increase in the rate of burial of organic carbon. This sequestering of carbon may have been caused by increased rates of sediment deposition, related to the onset of regression and the increase in erosion rates. The presence of siliciclastic detritus in the carbonate rocks from the correlative conformity interval at the Maynardville/Copper Ridge transition

is considered a consequence of sea-level lowering and an increase in the input of craton-derived sediment (Fig. 2). This supports the relationship between sea-level fall and the maximum positive carbon-isotope excursion (Fig. 3).

Removal of carbon from the ocean surface layer can cause a decline in atmospheric P_{CO_2} and subsequent global climatic cooling (Vincent and Berger 1985; Knoll et al. 1986; Marshall and Middleton 1990). This can potentially explain the link between the positive carbon-isotope excursion and the sea-level fall at the Sauk II/Sauk III boundary. The cause of this sea-level fall is unclear, given that the Cambrian was a time of little or no continental glaciation. The lack of evidence for glaciation, however, does not imply absence of climatic cooling during the excursion. The cooling event may not have caused glaciation because of the absence of continental land masses in polar regions during the Late Cambrian (Scotese and McKerrow 1990). Global climatic cooling can cause major oceanographic changes such as a destabilization in the oceanic density structure or ocean overturns that bring deep ^{13}C-depleted water to the surface (Wilde and Berry 1984). The end of the Late Cambrian carbon-isotope excursion can thus be related to climate-induced ocean mixing, coupled with oxidation of organic matter during a sea-level fall. Similar interpretations have been proposed for the late Proterozoic and Late Ordovician positive carbon-isotope shifts (Wilde and Berry 1984; Marshall and Middleton 1990; Kaufman et al. 1991; Derry et al. 1992).

Some of the Mesozoic and Cenozoic positive carbon-isotope shifts, however, coincide with sea-level maxima (Berger and Vincent 1986; Arthur et al. 1987; Jenkyns 1996). The association of high sea level and ^{13}C enrichment in the oceans has been attributed to a high accumulation rate of organic carbon in sediments on extensive shelf areas (Berger and Vincent 1986; Jenkyns 1996). A sea-level rise due to climate warming can accelerate the hydrologic cycle and intensify weathering. This would cause nutrient mobilization and an increase in organic productivity, which could in turn lead to increased carbon burial and a positive carbon-isotope excursion (Föllmi et al. 1994). On the other hand, Brasier (1992) noted that increased nutrient availability, an associated increase in organic productivity, and lowering of the $^{13}C/^{12}C$ ratio in the surface waters all occur during sea-level *fall* and increased terrestrial runoff. Such interpretations suggest that prominent changes in carbon cycling are likely to occur during *sea-level changes,* and that similar signals in the carbon-isotope record of marine carbonate can result from rather different controlling factors. Consequently, there is no unique explanation for changes in carbon cycling throughout the geologic record.

CONCLUSIONS

(1) Elevated $\delta^{13}C$ values of Upper Cambrian carbonate deposits in the southern Appalachians reflect an increase in the $^{13}C/^{12}C$ ratio of sea water as a consequence of a major perturbation in the global cycling of carbon.

(2) Comparison with coeval carbon-isotope excursions documented in biostratigraphically well-characterized successions elsewhere provides a means for improving the chronostratigraphic framework for the Upper Cambrian in the southern Appalachians.

(3) Superimposed on the secular trend are minor variations in $\delta^{13}C$ values that can be related to conditions during deposition and postdepositional diagenetic modifications.

(4) Comparison of $\delta^{13}C$ and $\delta^{18}O$ values between depositional and diagenetic phases provides unique insights into the type and extent of diagenetic modifications.

(5) The positive carbon-isotope excursion documented in this study is related to changes in the rate of burial of organic carbon, which in turn can be linked to changes in sea level, rates of sediment accumulation, ocean stratification, climate, and possibly rates of organic productivity.

(6) If carefully applied, studies of carbon-isotope variations provide a useful stratigraphic tool and serve as an indicator of the dynamics of global environmental changes.

ACKNOWLEDGMENTS

This study is a part of the first author's dissertation research at The University of Tennessee, Knoxville. This research was partially supported by a Geological Society of America research grant to BG, and Discretionary and Mobil Carbonate Research Funds at the Department of Geological Sciences, University of Tennessee. We are especially thankful for thoughtful reviews by P. Myrow, I. Fairchild, S.G. Driese, C.I. Mora, and an anonymous reviewer. Valuable insights were provided through discussions with K.J. Tobin, M.R. Saltzman, and R.L. Ripperdan. A.J. Caldanaro is thanked for field assistance and help with illustrations. Analyses were performed at the Stable Isotope Laboratory run by C.I. Mora at the Department of Geological Sciences, University of Tennessee, Knoxville.

REFERENCES

Anderson, T.F., and Arthur, M.A., 1983, Stable isotopes of oxygen and carbon and their application to sedimentologic and paleoenvironmental problems, *in* Arthur, M.A., Anderson, T.F., Kaplan, I.R., Veizer, J., and Land, L.S., eds., Stable Isotopes in Sedimentary Geology: SEPM, Short Course 10, p. 1-1–1-151.

Arthur, M.A., Schlanger, S.O., and Jenkyns, H.C., 1987, The Cenomanian–Turonian oceanic anoxic event, II. Palaeoceanographic controls on organic-matter production and preservation, *in* Brooks, J., and Fleet, A.J., eds., Marine Petroleum Source Rocks: Geological Society of London, Special Publication 26, p. 401–420.

Banner, J.L., and Hanson, G.N., 1990, Calculation of simultaneous isotopic and trace element variations during water–rock interaction with applications to carbonate diagenesis: Geochimica et Cosmochimica Acta, v. 54, p. 3123–3127.

Beauchamp, B., Oldershaw, A.E., and Krouse, H.R., 1987, Upper Carboniferous to Upper Permian ^{13}C-enriched primary carbonates in the Sverdrup Basin, Canadian Arctic: Comparison to coeval western North American ocean margins: Chemical Geology, Isotope Geoscience Section, v. 65, p. 391–413.

Berger, W.H., and Vincent, E., 1986, Deep-sea carbonates: Reading the carbon-isotope signal: Geologische Rundschau, v. 75, p. 249–269.

Bond, G.C., Kominz, G.C., and Grotzinger, J.P., 1988, Cambro-Ordovician eustasy: evidence from geophysical modeling of subsidence in Cordilleran and Appalachian passive margins, *in* Kleinspehn, K.L., ed., New Perspectives in Basin Analysis: New York, Springer-Verlag, p. 125–160.

Bond, G.C., Kominz, M.A., Steckler, M.S., and Grotzinger, J.P., 1989, Role of thermal subsidence, flexure, and eustasy in the evolution of early Paleozoic passive-margin carbonate platforms, *in* Crevello, P., Wilson, J.L., Sarg, J.F., and Read, J.F., eds., Controls on Carbonate Platform and Basin Development: SEPM, Special Publication 44, p. 39–61.

Brasier, M.D., 1992, Nutrient-enriched waters and the early skeletal fossil record: Geological Society of London, Journal, v. 149, p. 621–629.

Brasier, M.D., 1993, Towards a carbon isotope stratigraphy of the Cambrian system: potential of the Great Basin succession, *in* Hailwood, E.A., and Kidd, R.B., eds., High Resolution Stratigraphy: Geological Society of London, Special Publication 70, p. 341–359.

Brasier, M.D., Corfield, R.M., Derry, L.A., Rozanov, A.Yu., and Zhuravlev, A.Yu., 1994, Multiple $\delta^{13}C$ excursions spanning the Cambrian explosion to the Botomian crisis in Siberia: Geology, v. 22, p. 455–458.

Bridge, J., 1956, Stratigraphy of the Mascot–Jefferson City Zinc District, Tennessee: U.S. Geological Survey, Professional Paper 277, 74 p.

Calvert, S.E., Bustin, R.P., and Ingall, E.D., 1996, Influence of water column anoxia and sediment supply on the burial and preservation of organic carbon in marine shales: Geochimica et Cosmochimica Acta, v. 60, p. 1577–1593.

Carpenter, S.J., Lohmann, K.C, Holden, P., Walter, L.M., Huston, T.J., and Halliday, A.N., 1991, $\delta^{18}O$ values, $^{87}Sr/^{86}Sr$ and Sr/Mg ratios of Late Devonian abiotic marine calcite: Implications for the composition of ancient seawater: Geochimica et Cosmochimica Acta, v. 55, p. 1991–2010.

Charles, C.D., Wright, J.D., and Fairbanks, R.G., 1993, Thermodynamic influences on the marine carbon isotope record: Paleoceanography, v. 8, p. 691–697.

Claypool, G.E., and Kaplan, I.R., 1974, The origin and distribution of methane in marine sediments, *in* Kaplan, I.R., ed., Natural Gases in Marine Sediments: New York, Plenum Press, p. 99–140.

Coleman, M.L., and Raiswell, R., 1981, Carbon, oxygen and sulphur isotope variations in concretions from the Upper Lias of N.E. England: Geochimica et Cosmochimica Acta, v. 45, p. 329–340.

Derby, J.R., 1965, Paleontology and stratigraphy of the Nolichucky Formation in southeast Virginia and northeast Tennessee [unpublished Ph.D. thesis]: Virginia Polytechnic Institute and State University, Blacksburg, Virginia, 465 p.

Derry, L.A., Kaufman, A.J., and Jacobsen, S.B., 1992, Sedimentary cycling and environmental change in the Late Proterozoic: Evidence from stable and radiogenic isotopes: Geochimica et Cosmochimica Acta, v. 56, p. 1317–1329.

DesMarais, D.J., Cohen, Y., Nguyen, H., Cheatham, T., and Mu–oz, E., 1989, Carbon isotopic trends in the hypersaline ponds and microbial mats at Guerrero Negro, Baja California Sur, Mexico: Implications for Precambrian stromatolites, *in* Cohen, Y., and Rosenberg, E., eds., Microbial Mats, Physiological Ecology of Benthic Microbial Communities: American Society for Microbiology, p. 191–203.

EPSTEIN, S., GRAF, D.L., AND DEGENS, E.T., 1963, Oxygen isotope studies on the origin of dolomites, *in* Craig, H., Miller, S.L., and Wasserburg, G.J., eds., Isotopic and Cosmic Chemistry: Amsterdam, North-Holland, p. 169–180.

FAIRCHILD, I.J., MARSHALL, J.D., AND BERTRAND-SARFATI, J., 1990, Stratigraphic shifts in carbon isotopes from Proterozoic stromatolitic carbonates (Mauritania): Influences of primary mineralogy and diagenesis: American Journal of Science, v. 290-A, p. 46–79.

FÖLLMI, K.B., WEISSERT, H., BISPING, M., AND FUNK, H., 1994, Phosphogenesis, carbon-isotope stratigraphy, and carbonate-platform evolution along the Lower Cretaceous northern Tethyan margin: Geological Society of America, Bulletin, v. 106, p. 729–746.

FRIEDMAN, I., AND O'NEIL, J.R., 1977, Compilation of stable isotope fractionation factors of geochemical interest: U.S. Geological Survey, Professional Paper 440-KK, 12 p.

GALE, A.S., JENKYNS, H.C., KENNEDY, W.J., AND CORFIELD, R.M., 1993, Chemostratigraphy versus biostratigraphy: data from around the Cenomanian-Turonian boundary: Geological Society of London, Journal, v. 150, p. 29–32.

GAUTIER, D.L., AND CLAYPOOL, G.E., 1984, Interpretation of methanic diagenesis in ancient sediments by analogy with processes in modern diagenetic environments, *in* McDonald, D.A., and Surdam, R.C., eds., Clastic Diagenesis: American Association of Petroleum Geologists, Memoir 37, p. 111–123.

GLUMAC, B., 1997, Cessation of Grand Cycle deposition in the framework of passive margin evolution: controlling mechanisms and effects on carbonate deposition and diagenesis, Cambrian Maynardville Formation, southern Appalachians [unpublished Ph.D. thesis]: The University of Tennessee, Knoxville, 380 p.

GOERICKE, R., MONTOYA, J.P., AND FRY, B., 1994, Physiology of isotopic fractionation in algae and cyanobacteria, *in* Lajtha, K., and Michener, R.H., eds., Stable Isotopes in Ecology and Environmental Science: Boston, Blackwell, p. 187–221.

HOLSER, W.T., MAGARITZ, M., AND WRIGHT, J., 1986, Chemical and isotopic variations in the world ocean during Phanerozoic time, *in* Walliser, O.H., ed., Global Bio-Events: a critical approach: Berlin, Springer-Verlag, Lecture Notes in Earth Sciences, v. 8, p. 63–74.

HOWELL, B.F., BRIDGE, J., DEISS, C.F., EDWARDS, I., LOCHMAN, C., RAASCH, G.O., AND RESSER, C.E., 1944, Correlation of the Cambrian formations of North America: Geological Society of America, Bulletin, v. 55, p. 993–1003.

HUDSON, J.D., AND ANDERSON, T.F., 1989, Ocean temperatures and isotopic compositions through time: Royal Society of Edinburgh, Transactions, Earth Sciences, v. 80, p. 183–192.

IRWIN, H., CURTIS, C., AND COLEMAN, M., 1977, Isotopic evidence for source of diagenetic carbonates formed during burial of organic sediments: Nature, v. 269, p. 209–213.

IYER, S.S., BABINSKI, M., KROUSE, H.R., AND CHAMELE, F., 1995, Highly ^{13}C-enriched carbonate and organic matter in the Neoproterozoic sediments of the Bambui Group, Brazil, *in* Knoll, A.H., and Walter, M., eds., Neoproterozoic Stratigraphy and Earth History: Precambrian Research, v. 73, p. 271– 282.

JAMES, N.P., AND STEVENS, R.K., 1986, Stratigraphy and correlation of the Cambro-Ordovician Cow Head Group, western Newfoundland: Geological Survey of Canada Bulletin 366, 143 p.

JENKYNS, H.C., 1996, Relative sea-level change and carbon isotopes: data from the Upper Jurassic (Oxfordian) of central and Southern Europe: Terra Nova, v. 8, p. 75–85.

KAUFMAN, A.J., AND KNOLL, A.H., 1995, Neoproterozoic variations in the C-isotopic composition of seawater: stratigraphic and biogeochemical implications: Precambrian Research, v. 73, p. 27–49.

KAUFMAN, A.J., HAYES, J.M., KNOLL, A.H., AND GERMS, G.J.B., 1991, Isotopic compositions of carbonates and organic carbon from upper Proterozoic successions in Namibia: stratigraphic variation and the effects of diagenesis and metamorphism: Precambrian Research, v. 49, p. 301–327.

KAUFMAN, A.J., JACOBSEN, S.B., AND KNOLL, A.H., 1993, The Vendian record of Sr and C isotopic variations in seawater: Implications for tectonics and paleoclimate: Earth and Planetary Science Letters, v. 120, p. 409–430.

KAUFMAN, A.J., KNOLL, A.H., AND AWRAMIK, S.M., 1992, Biostratigraphic and chemostratigraphic correlation of Neoproterozoic sedimentary successions: Upper Tindir Group, northwestern Canada, as a test case: Geology, v. 20, p. 181–185.

KNOLL, A.H., GROTZINGER, J.P., KAUFMAN, A.J., AND KOLOSOV, P., 1995a, Integrated approaches to terminal Proterozoic stratigraphy: An example from the Olenek Uplift, northeastern Siberia: Precambrian Research, v. 73, p. 251–270.

KNOLL, A.H., HAYES, J.M., KAUFMAN, A.J., SWETT, K., AND LAMBERT, I.B., 1986, Secular variations in carbon isotope ratios from upper Proterozoic successions of Svalbard and East Greenland: Nature, v. 321, p. 832–838.

KNOLL, A.H., KAUFMAN, A.J., AND SEMIKHATOV, M.A., 1995b, The carbon-isotopic composition of Proterozoic carbonates: Riphean successions from Northwestern Siberia (Anabar massif, Turukhansk uplift): American Journal of Science, v. 295, p. 823–850.

KROOPNICK, P.M., 1985, The distribution of ^{13}C of ΣCO_2 in the world oceans: Deep-Sea Research, v. 32, p. 57–84.

LAND, L.S., 1980, The isotopic and trace element geochemistry of dolomite: the state of art, *in* Zenger, D.H., Dunham, J.B., and Ethington, R.L., eds., Concepts and Models of Dolomitization: Society of Economic Paleontologists and Mineralogists, Special Publication 28, p. 87–110.

LAZAR, B., AND EREZ, J., 1992, Carbon geochemistry of marine-derived brines: I. ^{13}C depletion due to intense photosynthesis: Geochimica et Cosmochimica Acta, v. 56, p. 335–345.

LOCHMAN-BALK, C., 1971, Cambrian of the craton, *in* Holland, E.R., ed., Cambrian of the New World, Lower Paleozoic Rocks of the World (Vol 1): New York, Wiley Interscience, p. 79–167.

LOHMANN, K.C, AND WALKER, J.C.G., 1989, The $\delta^{18}O$ record of Phanerozoic abiotic marine calcite cements: Geophysical Research Letters, v. 16, p. 319–322.

LUDVIGSEN, R., AND WESTROP, S.R., 1985, Three new Upper Cambrian stages for North America: Geology, v. 13, p. 139–143.

MAGARITZ, M., 1991, Carbon isotopes, time boundaries and evolution: Terra Nova, v. 3, p. 251–256.

MAGARITZ, M., KIRSCHVINK, J.L., LATHAM, A.J., ZHURAVLEV, A.YU., AND ROZANOV, A.YU., 1991, Precambrian/Cambrian boundary problem: Carbon isotope correlations for Vendian and Tommotian time between Siberia and Morocco: Geology, v. 19, p. 847–850.

MARSHALL, J.D., 1992, Climatic and oceanographic isotopic signals from the carbonate rock record and their preservation: Geological Magazine, v. 2, p. 143–160.

MARSHALL, J.D., AND MIDDLETON, P.D., 1990, Changes in marine isotopic composition and the late Ordovician glaciation: Geological Society of London, Journal, v. 147, p. 1–4.

MCKENZIE, J.A., 1981, Holocene dolomitization of calcium carbonate sediments from the coastal sabkhas of Abu Dhabi, U.A.E.: a stable isotope study: Journal of Geology, v. 89, p. 185–198.

NARBONNE, G.M., KAUFMAN, A.J., AND KNOLL, A.H., 1994, Integrated chemostratigraphy and biostratigraphy of the upper Windermere Supergroup (Neoproterozoic), Mackenzie Mountains, northwestern Canada: Geological Society of America, Bulletin, v. 106, p. 1281–1291.

OSLEGER, D.A., AND READ, J.F., 1993, Comparative analysis of methods used to define eustatic variations in outcrop: Late Cambrian interbasinal sequence development: American Journal of Science, v. 293, p. 157–216.

PALMER, A.R., 1965a, Biomere—A new kind of biostratigraphic unit: Journal of Paleontology, v. 39, p. 149–153.

PALMER, A.R., 1965b, Trilobites of the Late Cambrian Pterocephaliid Biomere in the Great Basin, United States: U.S. Geological Survey, Professional Paper 493, 103 p.

PALMER, A.R., 1971, The Cambrian of the Appalachian and eastern New England regions, eastern United States, *in* Holland, C.H., ed., Lower Paleozoic Rocks of the World: Cambrian of the New World (Vol. 1): New York, Wiley Interscience, p. 169–217.

PALMER, A.R., 1981, Subdivision of the Sauk sequence, *in* Taylor, M.E., ed., Short Papers for the Second International Symposium on the Cambrian system: U.S. Geological Survey, Open File Report 81-743, p. 160–163.

PELECHATY, S.M., KAUFMAN, A.J., AND GROTZINGER, J.P., 1996, Evaluation of $\delta^{13}C$ chemostratigraphy for intrabasinal correlation: Vendian strata of northeast Siberia: Geological Society of America, Bulletin, v. 108, p. 992–1003.

RASETTI, F., 1965, Upper Cambrian trilobite faunas of northeastern Tennessee: Smithsonian Miscellaneous Collections, v. 148, 140 p.

ROEDER, D., AND WITHERSPOON, W.D., 1978, Palinspastic map of east Tennessee: American Journal of Science, v. 278, p. 543–550.

ROMANEK, C.S., GROSSMAN, E.L., AND MORSE, J.W., 1992, Carbon isotopic fractionation in synthetic aragonite and calcite: Effects of temperature and precipitation rate: Geochimica et Cosmochimica Acta, v. 56, p. 419–430.

ROWELL, A.J., AND BRADY, M.J., 1976, Brachiopods and biomeres: Brigham Young University Geology Studies 23, p. 165–180.

SALTZMAN, M.R., 1996, Extinction and environmental change, Late Cambrian, Wyoming and Utah [unpublished Ph.D. thesis]: The University of California, Los Angeles, 169 p.

SALTZMAN, M.R., RUNNEGAR, B., AND LOHMANN, K.C, 1998, Carbon isotope stratigraphy of Upper Cambrian (Steptoean Stage) sequences of the eastern Great Basin: Record of a global oceanographic event: Geological Society of America, Bulletin, v. 110, p. 285–297.

SCHIDLOWSKI, M., AND AHARON, P., 1992, Carbon cycle and carbon isotope record: Geochemical impact of life over 3.8 Ga of Earth history, *in* Schidlowski, M., Golubić, S., Kimberley, M.M., McKirdy, D.M., and Trudinger, P.A., eds., Early Organic Evolution: Implications for Mineral and Energy Resources: New York, Springer-Verlag, p. 147–175.

SCOTESE, C.R., AND MCKERROW, W.S., 1990, Revised world maps and introduction, *in* McKerrow, W.S., and Scotese, C.R., eds., Palaeozoic Palaeogeography and Biogeography: Geological Society of London, Memoir 12, p. 1–24.

STILLER, M., ROUNICK, J.S., AND SHASHA, S., 1985, Extreme carbon-isotope enrichments in evaporating brines: Nature, v. 316, p. 434–435.

SURGE, D.M., SAVARESE, M., DODD, J.R., AND LOHMANN, K.C, 1997, Carbon isotopic evidence for photosynthesis in Early Cambrian oceans: Geology, v. 25, p. 503–506.

THICKPENNY, A., AND LEGGETT, J.K., 1987, Stratigraphic distribution and palaeo-oceanographic significance of European early Palaeozoic organic-rich sediments, *in* Brooks, J., and Fleet, A.J., eds., Marine Petroleum Source Rocks: Geological Society of London, Special Publication 26, p. 231–247.

VAHRENKAMP, V.C., 1996, Carbon isotope stratigraphy of the Upper Kharaib and Shuaiba Formations: Implications for the Early Cretaceous evolution of the Arabian Gulf Region: American Association of Petroleum Geologists, Bulletin, v. 80, p. 647–662.

VEIZER, J., 1983, Trace elements and isotopes in sedimentary carbonates, *in* Reeder, R.J., ed., Carbonates: Mineralogy and Chemistry: Mineralogical Society of America, Reviews in Mineralogy, v. 11, p. 265–299.

VINCENT, E., AND BERGER, W.H., 1985, Carbon dioxide and polar cooling in the Miocene: the Monterey hypothesis, *in* Sundquist, E.T., and Broecker, W.S., eds., The Carbon Cycle and Atmospheric CO_2: American Geophysical Union, Monograph 32, p. 455–468.

WADA, H., AND SUZUKI, K., 1983, Carbon isotopic thermometry calibrated by dolomite–calcite solvus temperatures: Geochimica et Cosmochimica Acta, v. 47, p. 697–706.

WALTERS, L.J., CLAYPOOL, G.E., AND CHOQUETTE, P.W., 1972, Reaction rates and δO^{18} variation for the carbonate–phosphoric acid preparation method: Geochimica et Cosmochimica Acta, v. 36, p. 129–140.

WEISSERT, H., 1989, C-isotope stratigraphy, a monitor of paleoenvironmental change: A case study from the early Cretaceous: Surveys in Geophysics, v. 10, p. 1–61.

WILDE, P., AND BERRY, W.B.N., 1984, Destabilization of the oceanic density structure and its significance to marine ''extinction'' events: Palaeogeography, Palaeoclimatology, Palaeoecology, v. 48, p. 143–162.

WINTER, B.L., AND KNAUTH, L.P., 1992, Stable isotope geochemistry of carbonate fracture fills in the Monterey Formation, California: Journal of Sedimentary Petrology, v. 62, p. 208–219.

Received 9 January 1998; accepted 24 May 1998.